A Neural Network Based Modeling Approach for A Piezoelectric-Actuated Stick-Slip Positioning Device

Long Cheng and Ang Wang
State Key Laboratory of Management and Control for Complex Systems
Institute of Automation, Chinese Academy of Sciences
Beijing 100190, China
University of Chinese Academy of Sciences
Beijing 100049, China
Email: long.cheng@ia.ac.cn

***Abstract*—Nano/micro-positioning has become a fundamental technology in many practical applications where piezoelectric actuators (PEAs) are widely used as the core component. However, the displacement range of PEAs is limited because of the intrinsic characteristics of the material. Therefore, the piezoelectric-actuated stick-slip device is developed, which have theoretically unlimited motion and high positioning precision. The dynamical model of the end-effector's displacement is of significance for its precise control. Due to the complicated stick-slip movement mode and the hysteresis nonlinearity existing in PEAs, modeling of the piezoelectric-actuated stick-slip device is a challenging task. In this paper, a piezoelectric-actuated stick-slip device is implemented first, which consists of one end-effector and one PEA. Then, instead of considering the end-effector and the PEA separately, the entire system is treated as a whole plant. Taking advantage of its strong approximation ability, a multilayer feedforward neural network is applied to describe the complicated nonlinear relation between the control input voltage of the PEA and the output displacement of the end-effector. In order to validate the effectiveness of the proposed modeling method, some experiments are carried out on a self-designed piezoelectric-actuated stick-slip prototype, which shows a satisfactory modeling performance (the maximum modeling error is less than 0.05 μm).**

Keywords*—Piezoelectric actuator, stick-slip principle, neural network, modeling.

I. Introduction

Recently, ultra-precision positioning has become a vital technology in advanced manufacturing. Piezoelectric actuators are the mostly adopted component for the ultra-precision positioning (nano/mirco-scale level) because they are characterized by the high stiffness and fast response. However, the motion range of piezoelectric actuators is usually limited. Taking one commercial product (P-753.1CD, Physik Instrumente, Karlsruhe, Germany) for example, its motion limit is up to 15μm, which cannot satisfy many practical applications. To deal with this challenge, the piezoelectric-actuated stick-slip device has been proposed. Based on the stick-slip principle, the end-effector can move on the upper surface of the PEA with theoretically unlimited motion range while still keep a relatively high positioning precision. The working principle of the piezoelectric-actuated stick-slip device is briefly introduced below. Interested readers are referred to the survey papers [1]–[3] for details.

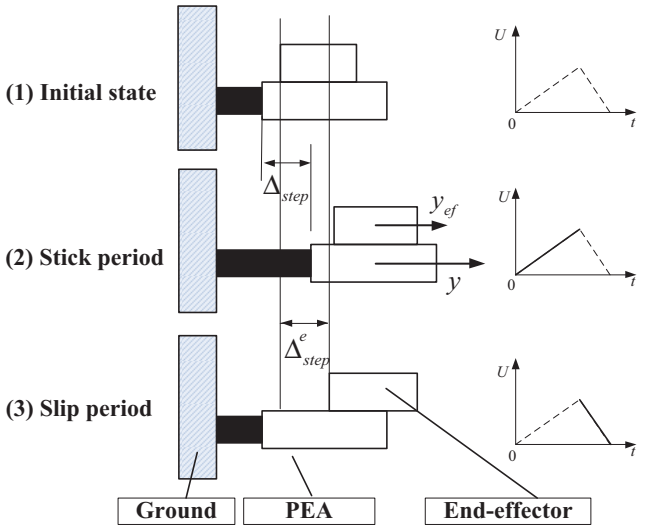

Fig. 1. Working principle of the piezoelectric-actuated stick-slip device [4].

The piezoelectric-actuated stick-slip device is usually composed of one PEA[1] and one end-effector. The end-effector is placed on the upper surface of the PEA and can move on the surface of the PEA. The motion of the end-effector usually includes three states: the initial state, the stick period and the slip period, which are shown in Fig. 1.

- *Initial state*: in this state, the entire piezoelectric-actuated stick-slip device remains at the resting state. There is no input voltage applied to the PEA and there is no relative motion between the PEA and the end-effector.
- *Stick period*: in this period, the control input voltage is applied to the PEA, which increases very slowly. This control effort can drive the PEA rightward to a displacement Δ_{step} with a low acceleration. Since the PEA's acceleration is very slow, the friction force between the end-effector and the PEA remains below the threshold of the static friction. In this case, the end-

[1]In Fig. 1, the PEA is described by the black box. A driving object (the white box) is also adhered to the PEA to increase the motion range of the end-effector. For the sake of simplicity, we treat the PEA and the driving object as a "big" PEA.

978-1-5386-2602-3/17/$31.00/ ©2017 IEEE

effector moves along the PEA to the same displacement Δ_{step} without any relative motion, which looks like that the end-effector is "stuck" on the surface of the PEA.

- *Slip period*: in this period, the input voltage of the PEA is rapidly decreased to zero. Then the PEA moves leftward to its initial position with a very high acceleration. The friction between the end-effector and the PEA goes beyond the static friction threshold and there is a relative motion between the end-effector and the PEA. The end-effector "slips" on the surface of the PEA. At the end of the slip period, the moving displacement of the end-effector is Δ^e_{step}.

From the above working principle, the positioning of the end-effector can be made by the following two control phases: the one-step control phase (coarse positioning) and the sub-step control phase (fine positioning). The one-step control phase is composed of one stick period and one slip period. By repeating the one-step control phase, the end-effector continuously moves on the surface of the PEA with a resolution of Δ^e_{step}. Therefore, the end-effector can have a theoretically unlimited motion range. For example, if the end-effector is required to move a displacement of L^e, then the one-step control phase should be repeated by $\lfloor L^e/\Delta^e_{step} \rfloor$ times ($\lfloor x \rfloor$ denotes the largest integer less than x). Following the one-step control phase, the positioning of the end-effector enters the sub-step control phase. In this phase, there are two control options. One is to increase the control input voltage very slowly such that the PEA has a very small acceleration and there is no relative motion between the PEA and the end-effector (like the stick period). Then by accurately positioning the PEA to a displacement of $L^e - \lfloor L^e/\Delta^e_{step} \rfloor \Delta^e_{step}$, the desired displacement L^e of the end-effector can be reached [4]. Another sub-step control approach is to allow the relative motion between the end-effector and the PEA. And use the advanced control algorithms to achieve the fine positioning $L^e - \lfloor L^e/\Delta^e_{step} \rfloor \Delta^e_{step}$ of the end-effector under the existence of relative motion.

By the aforementioned introduction, the ultra-precision control of the piezoelectric-actuated stick-slip device is mainly depended on two factors: one is the accurate positioning of PEAs; and the other is the relative motion between the end-effector and the PEA. There is a rich literature regarding the accurate positioning of PEAs. The positioning approach of PEAs can be roughly divided into three categories: the feedforward control approach, the feedback control approach and the feedforward-feedback control approach. The feedforward control approach is to obtain a dynamical model of PEAs first, then use the inversion of the PEA's model to compensate the dynamics of PEAs (ideally, cascading the PEA by the inversion of its dynamics leads to an unit mapping). The dynamical model of PEAs is usually dominated by the hysteresis nonlinearity. The hysteresis modeling method can be divided into the following types: the operator based model like the Preisach model [5] and the Prandtl-Ishlinskii model [6]; the differential equation physical model like the Duhem model [7] and the Bouc-Wen model [8]; and the data-driven based model like the neural network based model [9]–[11] and the fuzzy logic model [12], [13]. The feedback control approach can be further divided into the model-free control algorithm and the model-based control algorithm. The model-free control algorithm is designed without knowing the exact model information such as the active disturbance rejection control [14] and the fuzzy PID control [15]. Since the model information is utilized, the model-based control algorithm has a relatively high control performance, which includes the sliding mode control [16], [17], the H_∞ control [18], the robust adaptive control [19] and the model predictive control [20]–[22]. The third control strategy is the feedforward-feedback control which employs the feedforward control to compensate the hysteresis nonlinearity and uses the feedback control to suppress the external disturbances and model inaccuracy. Based on this control strategy, combinations of different inverse hysteresis models and different feedback control methods are studied [23]–[27]. The second factor affecting the control accuracy of piezoelectric-actuated stick-slip devices is the relative motion between the end-effector and the PEA, which is highly dependent on the friction. Many friction models (i.e., the Coulomb model, the viscous model, the Dahl model, the LuGre model and the elasto-plastic model) have been introduced in the literature [3]. Unfortunately, these friction models are usually nonlinear and very complicated which are rarely used in the controller design of the end-effector. To the best of the authors' knowledge, advanced control of piezoelectric-actuated stick-slip devices has not been well studied. The proportional control is still the dominant method of dealing with the friction and the hysteresis nonlinearity [3]. Some advanced results include the iterative learning control [28], the hybrid charge control [29] and the velocity compensation approach [30]. One recent paper proposes a neural network based control approach for the piezoelectric-actuated stick-slip device [31]. By collecting the displacement of the end-effector and the displacement of the PEA, the relatively motion between the PEA and the end-effector is approximated by a neural network model. Then the inversion of this neural network is calculated. Therefore, the desired displacement of the PEA can be determined by the desired displacement of the end-effector and the inversion of this neural network model. To achieve the desired displacement of PEAs, the model predictive control approach is employed. It is obvious that the controller proposed in [31] treats the PEA and the end-effector separately. It is interesting to investigate whether it is possible to find the relationship between the displacement of the end-effector and the control input voltage of the PEA directly, which gives the motivation of the study carried out in this paper.

This paper proposes a neural network based modelling approach for the piezoelectric-actuated stick-slip device. Different from the existing methods built on various friction models, the proposed method treats the piezoelectric-actuated stick-slip device as a black box and directly uses the data-driven approach to characterize the input-output relationship of the device. By collecting the input-output data of the device through experiments, a multi-layer feedforward neural network is trained to approximate the relationship between the displacement of the end-effector and the PEA's control input voltage. Compared to the previous result [31], the proposed modeling approach does not need to know the displacement of the PEA. Furthermore, the model predictive control approach can be easily designed by this neural network based model, while the controller proposed in [31] should know the inversion of the neural network to determine the desired displacement

of the PEA.

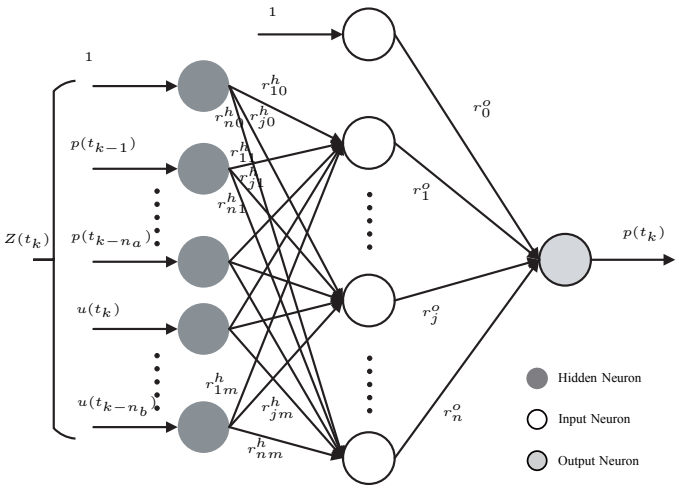

Fig. 2. Structure of the three-layer feedforward neural network for modeling the piezoelectric-actuated stick-slip device [31].

The rest of this paper is organized as follows. Section II explains how to model the piezoelectric-actuated stick-slip device by neural networks. Experimental results are presented in Section III and the hardware implementation of the PEA's controller is introduced in details. Section IV concludes this paper with the final remark.

II. Neural Network Based Modelling Approach

Borrowing the idea proposed in [20], [22], it can be assumed that the input-output relationship of the piezoelectric-actuated stick-slip device can be determined by the following "nonlinear auto-regressive moving average with exogenous inputs" structure

$$p(t_k) = \mathcal{F}\big(p(t_{k-1}), \cdots, p(t_{k-n_a}), u(t_k), \cdots, u(t_{k-n_b})\big), \tag{1}$$

where $p(t_k)$ denotes the displacement of the end-effector at t_k and $u(t_k)$ is the control input voltage of the PEA at t_k. n_a and n_b are positive integers representing the displacement lag and the input lag, respectively. n_a and n_b should be determined by the identification approach through experiments.

Due to the function approximation ability, the multi-layer feedforward neural network has been widely adopted to approximate the unknown function. This paper adopts the neural network shown in Fig. 2 to implement the "nonlinear auto-regressive moving average with exogenous inputs" mapping defined by (1).

$$p(t_k) = W^o \overline{\sigma}(W^h Z(t_k)), \tag{2}$$

where $W^h \in \Re^{(m+1)\times n}$ is the weight matrix between the input layer and the hidden layer. It is assumed that there are n neurons in the hidden layer. $Z(t_k) = \big(1, p(t_{k-1}), \cdots, p(t_{k-n_a}), u(t_k), \cdots, u(t_{k-n_b})\big)^T$ and $m = n_a + n_b + 1$. $W^o \in \Re^{1\times(n+1)}$ is the weight matrix between the hidden layer and the output layer; $\overline{\sigma}(W^h Z(t_k)) = \big(1, \sigma(W^h_{r_1} Z(t_k)), \sigma(W^h_{r_2} Z(t_k)), \cdots, \sigma(W^h_{r_n} Z(t_k))\big)^T \in \Re^{n+1}$ ($W^h_{r_i}$ represents the ith row of matrix W^h). $\sigma(\cdot)$ denotes the tangent sigmoid function, which is the activation function of the neuron in the hidden layer. For the neurons in the input layer and the output layer, the activation functions are the unit mapping.

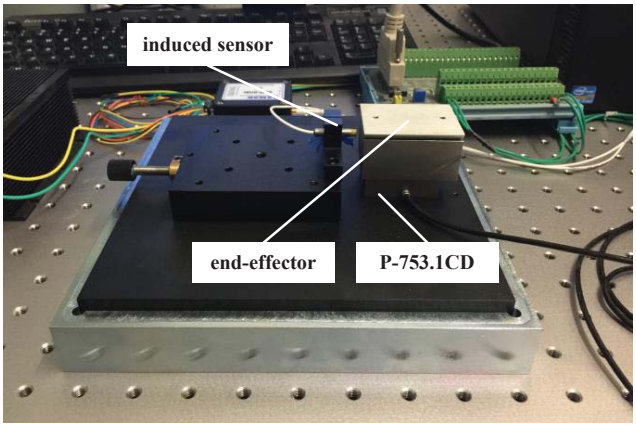

Fig. 3. The prototype of the piezoelectric-actuated stick-slip device developed in [31].

Through experiments, the input-output data pair $(Z(t_k), p(t_k))$ can be measured. Then, the neural network defined by (2) can be trained by the Levenberg-Marquardt algorithm.

III. Experimental Results

To verify the proposed modelling approach, the piezoelectric-actuated stick-slip prototype developed in [31] is employed for the experiment. This prototype is composed of one PEA (P-753.1CD, Physik Instrumente, Karlsruhe, Germany) and an end-effector. The end-effector is vertically placed on the PEA. The contact surface between the PEA and the end-effector is of the "V-shape" where the polished silicon wafers are adhered. Details about this prototype can be found in [31]. It should be noted that the commercial voltage controller (E-665.CR, Physik Instrumente) of the PEA used in the prototype has been replaced by a self-developed controller whose working frequency (800Hz) is much higher than the commercial one (less than 250Hz). The detail of this self-developed controller is introduced in the following subsection.

A. Design of the Self-Developed Controller of PEAs

The designed controller consists of the power supply module, control module and voltage amplifier.

1) Power Supply Module: Power supply module provides a stable direct current power source for the controller, where 3.3V, ±5V, ±15V and 150V voltages are needed. Considering the diversity of the power supply voltages, adjustable positive and negative DC power supply circuits are designed. 3-terminal adjustable regulator LM317 is selected as the core component of the adjustable positive DC power supply circuit because of its wide output-voltage range (1.25V to 37V) and high output current (greater than 1.5A). Similarly, 3-terminal adjustable regulator LM337 is chosen for the adjustable negative DC power supply circuit, which is capable of supplying -1.5A output current over an voltage range from -1.2V to -37V.

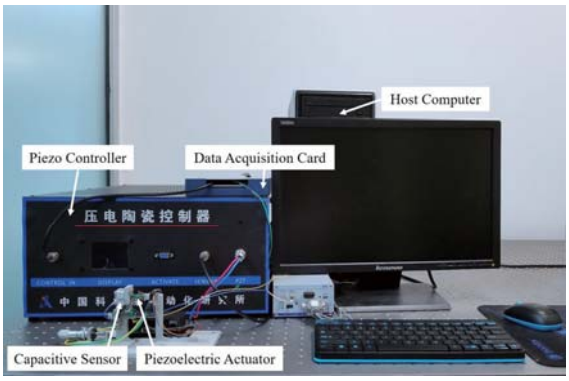

Fig. 4. The self-developed controller for PEAs.

Supply voltages of 3.3V, ±5V and ±15V are obtained by adjusting the resistor in the circuit. Supply voltage of 150V and the input voltage of the adjustable DC power supply circuits are provided by commercial power supply products.

2) Control Module: Control module is responsible for generating control voltage, collecting signals from the displacement sensor of the PEA and communicating with host computer, which is composed of the microcontroller unit (MPU), digital-to-analog converter (DAC) and analog-to-digital converter (ADC). 32-bit microcontroller STM32F407 (STMicroelectronics) is selected as the MCU because of its abundant interfaces and ease of use. A complete 16-bit D/A converter AD669 (Analog Devices, Inc) and a high precision ±10V external voltage reference AD688 are utilized to design DAC module. The core components of ADC module are 16-bit resolution, 500kSPS throughput A/D converter AD7693 (Analog Devices, Inc) and high-performance 5V voltage reference AD586. Both of DAC and ADC are well-designed to fully satisfy the system demand.

3) Voltage Amplifier: Voltage amplifier is the key module of the piezoelectric nanopositioning system, which amplifies the small voltage and directly drives the piezoelectric actuators. A composite circuit structure with two operational amplifiers is adopted to design a high-power high-frequency voltage amplifier. With the expected output voltage range from 0V to 120V and the maximum output current of 1A, PA96 (300V, 1.5A, Apex Microtechnology) is selected as the power operational amplifier. In order to reduce the input offset voltage, the precision amplifier ADA4638-1 is applied as the preamplifier. It's noted that piezoelectric actuators are equivalent to capacitive loads, which increase the difficulty of the circuit design. Therefore, the phase compensation is taken into consideration to ensure the stability of the voltage amplifier. The maximum working frequency can be calculated by

$$f = \frac{I_o}{2\pi C V_o},$$

where I_o is the output current, V_o is the output voltage, and C is the equivalent capacitance of piezoelectric actuators. When working at the state of $I_o = 1A$, $V_o = 120V$ and $C = 1.4\mu f$, the working frequency f is up to 947Hz, and higher working frequency is achievable if the output voltage or the equivalent capacitance is small.

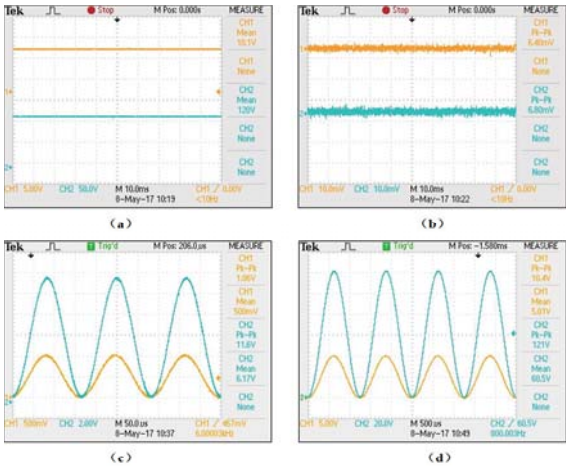

Fig. 5. Controller performance test: (a) DC voltage; (b) static ripple; (c) sinusoidal output with low peak-to-peak voltage; (d) sinusoidal output with high peak-to-peak voltage. (Tektronix TDS 2024C digital oscilloscope)

4) System Synthesis and Performance Testing: After all the module have been designed, the overall controller is obtained, which is shown in Fig. 4. Extensive experiments are conducted to test the performance of the designed controller. Figures 5(a) and 5(b) illustrate that the static ripple is below 10mv even at the situation of the maximum output voltage, which means that the voltage amplifier has a very high precision. It can be found in Figs. 5(c) and 5(d) that 800Hz sinusoidal output voltage is achieved with a peak-to-peak voltage of 121V, and for a sinusoidal output with 11.6V peak-to-peak voltage, the working frequency is up to 6KHz.

B. Verification of the Proposed Modelling Approach

First, the time-lags n_a and n_b should be determined. Various experiments on different n_a and n_b have been conducted. The experimental result is given in Table I, from which it can be seen that the best choice of n_a and n_b is $n_a = 2$ and $n_b = 2$.

TABLE I. EXPERIMENTS ON DETERMINING THE THE OUTPUT LAG n_a AND THE INPUT LAG n_b.

n_a	n_b	Root of mean square error (μm)	Maximum error (μm)	Minimum error (μm)
0	1	0.6218	0.5709	-1.0952
0	2	0.8546	0.2089	-1.5302
0	3	0.8984	0.2195	-1.4743
0	5	0.8650	0.0569	-1.5556
1	1	0.1187	0.1966	-0.2421
1	2	0.0083	0.0649	-0.0542
1	3	0.0066	0.0697	-0.0657
1	5	0.0055	0.0540	-0.0589
2	1	0.0084	0.1018	-0.0499
2	2	0.0050	0.0281	-0.0203
2	3	0.0064	0.0339	-0.0403
2	5	0.0077	0.0297	-0.0439
3	1	0.0072	0.0734	-0.0939
3	2	0.0065	0.0360	-0.0304
3	3	0.0075	0.0574	-0.0381
3	5	0.0095	0.0469	-0.0743
5	1	0.0084	0.0506	-0.0486
5	2	0.0052	0.0651	-0.0712
5	3	0.0054	0.0264	-0.0284
5	5	0.0107	0.0440	-0.0437

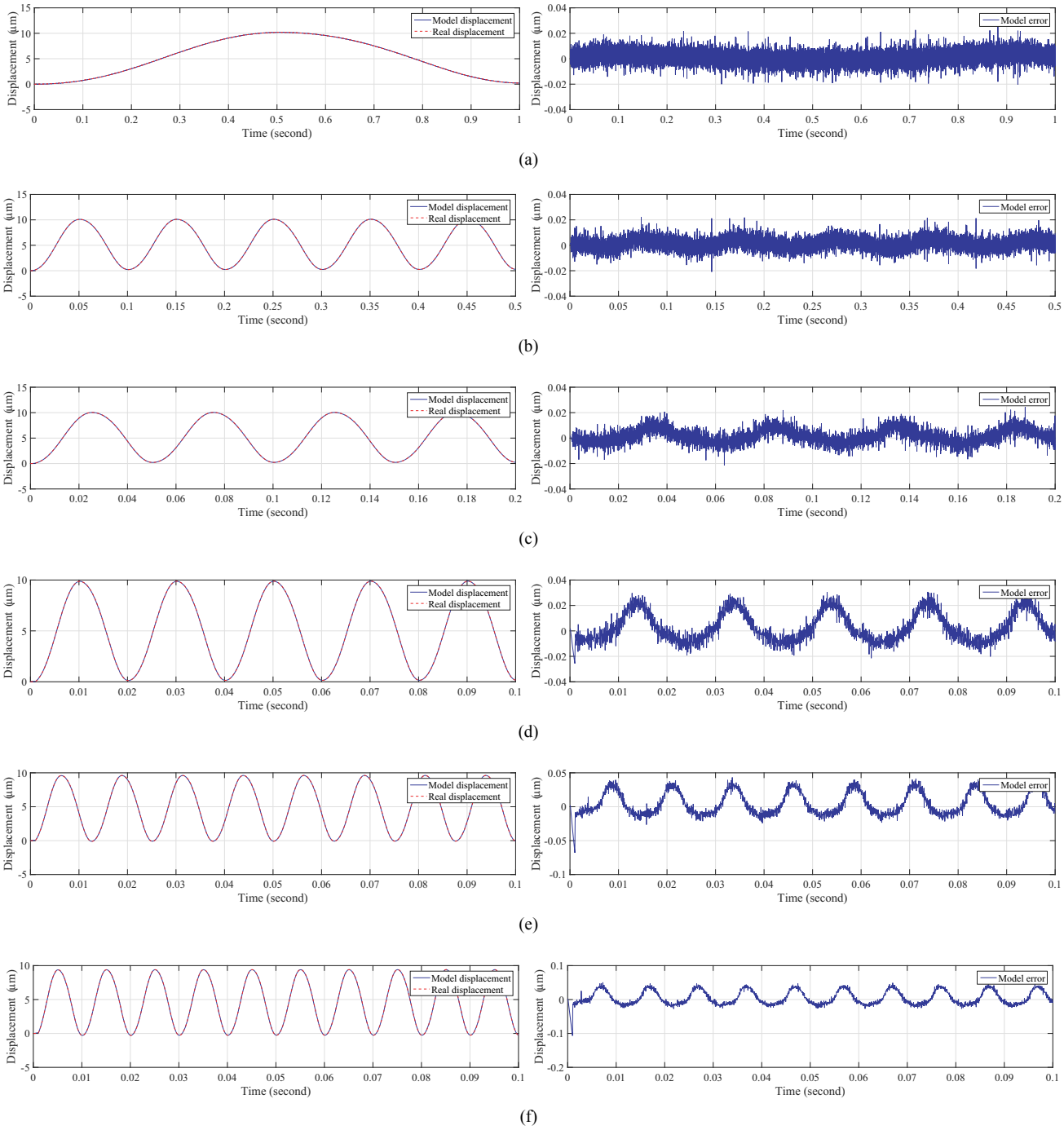

Fig. 6. Performance verification of the proposed modelling approach: (a) f = 1Hz; (b) f = 10Hz; (c) f = 20Hz; (d) f = 50Hz; (e) f = 80Hz; (f) f = 100Hz.

Second, the modelling performance of the proposed approach is verified. The input voltage of the PEA is set as the following references

$$u(t) = 4\sin(2\pi f t - \pi/2) + 4,$$

where the frequency f is set to be 1Hz, 10Hz, 20Hz, 50Hz, 80Hz and 100Hz, respectively. The experimental results are given in Fig. 6. It can be seen from the experiments that the maximum modelling error is smaller than 50nm, which is satisfactory for many practical applications.

IV. Conclusion

This paper proposes a neural network based modelling approach for the piezoelectric-actuated stick-slip device. The proposed approach treats the PEA and the end-effector as a whole and directly uses the input (the control input voltage of the PEA) and the output (the displacement of the end-effector) of the device to train the neural network. The advantage of this modelling approach can avoid the complicated friction models and there is no need to measure the displacement of the PEA. Some experiments have been made to determine the structure

of the neural network and verify the modelling performance. According to the experimental results, the maximum modelling error is within 50nm, which can meet the requirement of many nanopositioning applications. For the future work, more efforts are to be made towards designing the advanced controller for the piezoelectric-actuated stick-slip device. Since the neural network based model has been obtained, the model predictive controller is expected to have a good control performance by the previous results [22], [31], which is to be verified in the future.

ACKNOWLEDGMENT

This work was supported in part by the National Natural Science Foundation of China under Grants 61422310, 61633016, 61370032 and 61421004; the Beijing Natural Science Foundation under Grant 4162066.

REFERENCES

[1] Z.M. Zhang, Q. An, J.W. Li, and W.J. Zhang, "Piezoelectric friction-inertia actuator – a critical review and future perspective," *International Journal of Advanced Manufacturing Technology*, vol. 62, no. 5, pp. 669–685, 2012.

[2] M. Hunstig, "Piezoelectric inertia motors – a critical review of history, concepts, design, applications and perspectives," *Actuators*, vol. 6, no. 1, DOI: 10.3390/act6010007, 2017.

[3] Y.F. Liu, X.H. Hu, Z.M. Zhang, L. Cheng, Y. Lin, and W.J. Zhang, "Modeling and control of piezoelectric inertia-friction actuators: review and future research directions," *Mechnical Sciences*, vol. 6, pp. 95–107, 2015.

[4] W. Liu, L. Cheng, C. Zhou, Z.-G. Hou and M. Tan, "Neural-network based model predictive control for piezoelectric-actuated stick-slip micro-positioning devices," in *Proceedings of IEEE/ASME International Conference on Advanced Intelligent Mechatronics*, Banff, Canada, July 2016, pp. 1312–1317.

[5] Z. Li, X. Zhang, Y. Su, and T. Chai, "Nonlinear control of systems preceded by Preisach hysteresis description: a prescribed adaptive control approach," *IEEE Transactions on Control Systems Technology*, vol. 24, no. 2, pp. 451–460, 2016.

[6] G. Gu, L. Zhu, and C. Su, "Modeling and compensation of asymmetric hysteresis nonlinearity for piezoceramic actuators with a modified Prandtl-Ishlinskii model," *IEEE Transactions on Industrial Electronics*, vol. 61, no. 3, pp. 1583–1595, 2014.

[7] O. Ruiyue and B. ayawardhana, "Absolute stability analysis of linear systems with Duhem hysteresis operator," *Automatica*, vol. 50, no. 7, pp. 1860–1866, 2014.

[8] D. Habineza, M. Rakotondrabe, and Y. Le Gorrec, "Bouc-Wen modeling and feedforward control of multivariable hysteresis in piezoelectric systems: application to a 3-DoF piezotube scanner," *IEEE Transactions on Control Systems Technology*, vol. 23, no. 5, pp. 1797–1806, 2015.

[9] R. Dong, Y. Tan, H. Chen, and Y. Xie, "A neural networks based model for rate-dependent hysteresis for piezocermaic actuators," *Sensors and Acuators A: Physical*, vol. 143, no. 2, pp. 370–376, 2008.

[10] X. Zhao and Y. Tan, "Neural network based identification of Preisach-type hysteresis in piezoelectric actuator using hysteretic operator," *Sensors and Acuators A: Physical*, vol. 126, no. 2, pp. 306–311, 2006.

[11] W. Liu, L. Cheng, Z.-G. Hou, and M. Tan, "An inversion-free model predictive control with error compensation for piezoelectric actuators," in *Proceedings of the 2015 American Control Conference*, Chicago IL, USA, July 2015, pp. 5489–5494.

[12] W. Liu, L. Cheng, H. Wang, Z.-G. Hou, and M. Tan, "An inversion-free fuzzy predictive control for piezoelectric actuators," in *Proceedings of the 27th Chinese Control and Decision Conference*, Qingdao China, May 2015, pp. 959–964.

[13] P. Li, F. Yan, C. Ge, X. Wang, L. Xu, J. Guo, and P. Li, "A simple fuzzy system for modelling of both rate-independent and rate-dependent hysteresis in piezoelectric actuators," *Mechanical Systems and Signal Processing*, vol. 36, no. 1, pp. 182–192, 2013.

[14] W. Liu, L. Cheng, Z.-G. Hou, and M. Tan, "An active disturbance rejection controller with hysteresis compensation for piezoelectric actuators," in *Proceedings of the 12th World Congress on Intelligent Control and Automation*, Guilin, China, June 2016, pp. 2148–2153.

[15] A. Rebai, K. Guesmi, and B. Hemici, "Design of an optimized fractional order fuzzy PID controller for a piezoelectric actuator," *Control Engineering and Applied Informatics*, vol. 17, no. 3, pp. 41–49, 2015.

[16] J.Y. Peng, and X.B. Chen, "Integrated PID-based sliding mode state estimation and control for piezoelectric actuators," *IEEE/ASME Transactions on Mechatronics*, vol. 19, no. 1, pp. 88–99, 2014.

[17] Q. Xu, "Digital sliding mode control of piezoelectric micropositioning system based on input-output model," *IEEE Transactions on Industrial Electronics*, vol. 61, no. 10, pp. 5517–5526, 2014,

[18] C.-L. Hwang and S.-Y. Han, "Fuzzy mixed H_2/H_∞ optimization-based decentralized model reference control and application to piezo-driven XY table systems," *IEEE Transactions on Fuzzy Systems*, vol. 15, no. 2, pp. 145–160, 2007.

[19] H.C. Liaw and B. Shirinzadeh, "Robust adaptive constrained motion tracking control of piezo-actuated flexure-based mechanisms for micro/nano manipulation," *IEEE Transactions on Industrial Electronics*, vol. 58, no. 4, pp. 1406–1415, 2011.

[20] L. Cheng, W. Liu, Z.-G. Hou, J. Yu, and M. Tan, "Neural network based nonlinear model predictive control for piezoelectric actuators," *IEEE Transactions on Industrial Electronics*, vol. 62, no. 12, pp. 7717–7727, 2015.

[21] W. Liu, L. Cheng, J. Yu, Z.-G. Hou, and M. Tan, "An inversion-free predictive controller for piezoelectric actuators based on a dynamic linearized neural network model," *IEEE/ASME Transactions on Mechatronics*, vol. 21, no. 1, pp. 214–226, 2016.

[22] L. Cheng, W. Liu, Z.-G. Hou, T. Huang, J. Yu, and M. Tan, "An adaptive Takagi-Sugeno model based fuzzy predictive controller for piezoelectric actuators," *IEEE Transactions on Industrial Electronics*, vol. 64, no. 4, pp. 3048–3058, 2017.

[23] L. Liu, K.K Tan, and T.H. Lee, "Multirate-based composite controller design of piezoelectric actuators for high-bandwidth and precision tracking," *IEEE Transactions on Control Systems Technology*, vol. 22, no. 2, pp. 816–821, 2014.

[24] Y. Cao, L. Cheng, X.B. Chen, and J.Y. Peng, "An inversion-based model predictive control with an integral-of-error state variable for piezoelectric actuators," *IEEE/ASME Transactions on Mechatronics*, vol. 18, no. 3, pp. 895–904, 2013.

[25] M. Edardar, X.B. Tan, and H.K. Khalil, "Designand analysis of sliding mode controller under approximate hysteresis compensation," *IEEE Transactions on Control Systems Technology*, vol. 23, no. 2, pp. 598–608, 2014.

[26] A. Wang and L. Cheng, "A composite controller for piezoelectric actuators with model predictive control and hysteresis compensation," in *Proceedings of 2017 International Conference on Life System Modeling and Simulation and 2017 International Conference on Intelligent Computing for Sustainable Energy and Environment*, Nanjing, China, September 22–24, 2017, *Springer Communications in Computer and Information Science*, vol. 763, pp. 740–750.

[27] A. Wang and L. Cheng, "An adaptive fuzzy predictive controller with hysteresis compensation for piezoelectric actuators," submitted to *Congnitive Computation* for possible publication, 2017.

[28] Q. Zou, C.V. Giessen, J. Garbini, and S. Devasia, "Precision tracking of driving wave forms for inertial reaction devices," *Review of Scientific Instruments*, vol. 76, pp. 023701-023709, 2005.

[29] M. Spiller and Z. Hurak, "Hybrid charge control for stick-slip piezoelectric actuators," *Mechatronics*, vol. 21, no. 1, pp. 100–108, 2011.

[30] S.H. Chao, J.L. Garbini, W.M. Dougherty, and J.A. Sidles, "The design and control of a three-demensional piezoceramic tube scanner with an inertial slider," *Review of Scientific Instruments*, vol. 77, pp. 063710-063717, 2006.

[31] L. Cheng, W. Liu, C. Yang, Z.-G. Hou, T. Huang, and M. Tan, "Neural network based modeling and control of piezoelectric-actuated stick-slip devices," *IEEE Transactions on Industrial Electronics*, DOI: 10.1109/TIE.2017.2740826, 2017.